

A COMPUTER METHOD OF UNDERSTANDING OCULAR FUNDUS IMAGES

KOICHIRO AKITA and HIDEKI KUGA

Systems Science Division, Central Research Laboratory, Mitsubishi Electric Corpn.,
80 Nakano, Minamishimizu, Amagasaki, Japan 661

(Received 31 July 1981, in revised form 1 December 1981, received for publication 23 December 1981)

Abstract—We have studied some fundamental problems towards the understanding of color ocular fundus images which are used in the mass diagnosis of adult diseases such as hypertension and diabetes

These problems are the extraction of blood vessels from the retinal background, the recognition of arteries and veins, the detection and analysis of peculiar regions such as hemorrhages, exudates, optic discs and arterio-venous crossings

We propose a computer method for each of these problems and show some experimental results

Ocular fundus images Chromatic analysis Feature extraction Description of vessel networks
Relaxation labeling Pattern recognition Optic discs Hemorrhages

1 INTRODUCTION

Color ocular fundus images are used in the mass diagnosis of adult diseases such as hypertension and diabetes^(1, 2) Since photographing them is simple and cheap they can be used, once an automated analysis of them is developed, together with chest X-rays, for mass health management There are a few previous examples of computer analysis of ocular fundus images McCormich *et al*⁽³⁾ have developed a television ophthalmoscope image acquisition and display system, and applied it to fundus reflectometric measurements

Tamura *et al*⁽⁴⁾ analyzed fluorescence fundus angiograms They measured the areas of fluorescein leaks at various time intervals and investigated the correlation with the change of symptoms Tanaka and Tanaka⁽⁵⁾ analyzed the structural properties of the vascular system in making larger mosaic fundus images For color ocular fundus photographs, Nagin

and Schwartz⁽⁶⁾ applied some image processing techniques to analyze optic discs A global histogram analysis, local boundary tracking and a relaxation method for pixel labeling were used to make clear the condition of the discs Yamamoto *et al*⁽⁷⁾ investigated the possibility of automatic analysis of arterio-venous crossing phenomena But their method was interactive in the sense that they indicated the cross-points manually before the computer analysis

In this paper we propose some computer methods for examining blood vessel networks and for detecting and analyzing peculiar regions in color ocular fundus images such as hemorrhages, exudates, optic discs and arterio-venous crossings, some of which are shown in Fig 1

For the recognition of line segments of arteries/veins in the vessel networks we show an initial labeling scheme and how to apply the relaxation method together with its verification process This is a new approach which was suggested by Akita and Kuga^(8, 9)

For the detection of hemorrhages and exudates we define loop-composable sets of edge segments which are selected from region boundaries

In order to locate optic discs we define a parent-child relationship between blood vessel segments and propose an algorithm that traces vessel tree branchings back to the roots

An automatic method of analyzing arterio-venous crossings is suggested

The experimental results of these procedures are also presented

2 UNDERSTANDING BLOOD VESSEL NETWORKS

The color ocular fundus images are taken on 35 mm color reversal films by a fundus camera

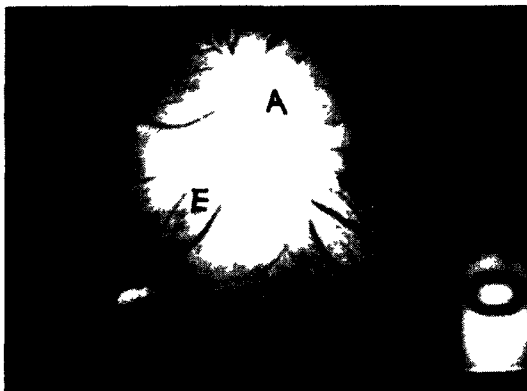


Fig 1 Peculiar regions in a color ocular fundus image A, Optic disc, B, arterio-venous crossing, C, hemorrhage, D, exudate, E, copper wire

In our experiment they were scanned by a drum scanner with a sampling pitch of 50 μm, and the photo density was quantized to 256 levels in each primary color

$$D_i = C \log \frac{\int J(\lambda) f_i(\lambda) d\lambda}{\int J(\lambda) f_i(\lambda) \delta(\lambda) d\lambda}, \quad i = \text{red, green, blue,}$$

where

- λ = wavelength,
- J(λ) = spectral energy distribution of light source,
- δ(λ) = spectral transmittance of film,
- f_i(λ) = spectral sensitivity of receiver,
- C = 255/2

A normal fundus image consists of four main portions, retina, disc, artery and vein. We plotted the chromatic information of the digitized data in the sample areas of each portion onto the UCS color coordinate system (u, v, V)⁽¹⁰⁾. From the analysis of distributions in (u, v, V) space as shown in Fig 2, we have acquired the following signal level knowledge⁽¹⁵⁾

- (1) The chromatic information of fundus images is approximately represented by the u-coordinate and the retina is roughly separated from blood vessels in this coordinate

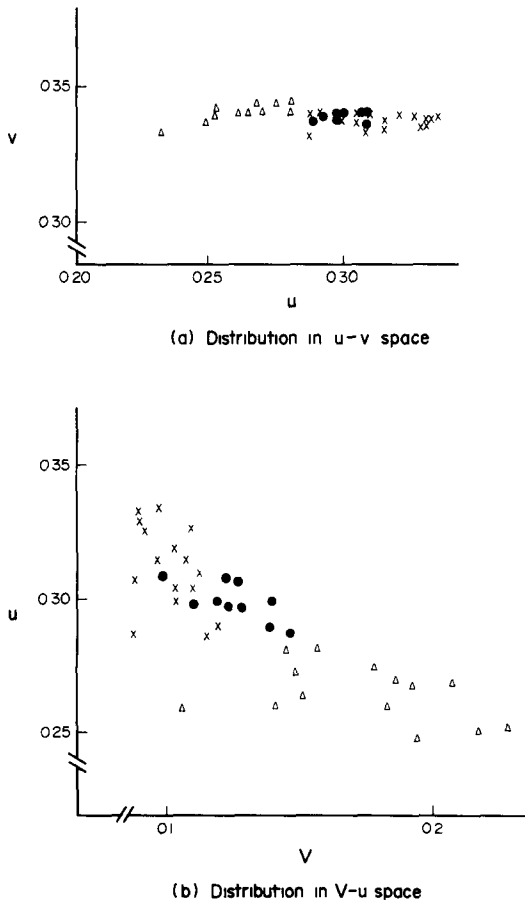


Fig 2 Chromatic analysis in (u, v, V) space x, Vein, ●, artery, Δ, retina

- (2) Arteries and veins cannot be completely distinguished in any coordinate, but if we limit the area in the image, then the V-(intensity) values are useful for discriminating arteries from veins. Henceforth we will use u-component images to extract vessels and use the average intensity (gray level) difference to show, in some local area, whether there are the same kind of vessels or not.

The analysis tells us that the labeling of blood vessels requires not only the signal level knowledge mentioned above, but also physical level knowledge⁽¹⁵⁾ on blood vessel networks

2.1 Extraction and description of blood vessel patterns

Since the ordinary global thresholding methods fail to extract blood vessels, other algorithms that take the shape characteristics of them into account are required. There are some line detection or ridge following algorithms which are often used to find linear features in LANDSAT images. We applied one of them⁽¹¹⁾ to the extraction of blood vessels from u-component images. The small blobs were excluded as noise. An example is shown in Fig 5(b). The spatial distribution or the state of blood vessels, such as branching, crossing and meandering, is simply represented by the pattern of their medial axes or skeletons. The direct results of thinning binary blood vessel images contain small circles, isolated points and prickles that act as noises. We first eliminate them. An example of this process is shown in Fig 5(c). Next, in order to analyze blood vessel networks, we detect characteristic points and line up line segments. We define three kinds of characteristic points: end-point, branch-point and cross-point. A line segment is defined as a segment of medial axis whose head and tail are characteristic points. Therefore, there are nine situations of a line segment.

In each line segment the terminal point which first appears when scanning from upper left to lower right will be called the head point (H Pt.) and the other one the tail point (T Pt.)

Several parameters on a characteristic point and a line segment are measured and are written into the characteristic points list (CP-LIST) and the line segments list (LS-LIST), respectively. These lists are very useful in activating the physical level knowledge which will be referred to later.

CP-LIST on I-th characteristic point (C Pt)

- (1) C Pt number = I, (2) X-coordinate, (3) Y-coordinate, (4) kind of C Pt, (5)–(9) for processing use, (10) number of the other C Pt on 1st line segment connected to I, (11) number of 1st line segment connected to I, (12), (14) and (16) similar to (10), (13), (15) and (17) similar to (11).

LS-LIST on J-th line segment

- (1) H Pt number, (2) T Pt number, (3) length, (4) angle between J and X-axis at H.Pt, (5) angle between J and X-axis at T Pt, (6) average intensity, (7) average vessel caliber around J, (8) and (9) for

processing use; (10) sign indicating the tracing direction of chain code, (11)–(1024) chain code

2.2 Recognition of arteries and veins

Let us label each line segment of a blood vessel network as either an artery or a vein. In Akita and Kuga⁽⁸⁾ we proposed a deterministic procedure and suggested that a relaxation method^(1,2) might also be applied. Here we utilize it.

First, a few segments which satisfy a certain constraint are picked up and discriminated as arteries or veins. This is the stage of initial labeling. The remaining unknown ones are labeled by the relaxation method. Finally, as a verification process, the label of each line segment is checked and corrected so as to minimize the total number of labeling contradictions.

The most powerful physical level knowledge that is used at this stage is as follows:

- (1) arteries (veins) branch off only from arteries (veins),
- (2) arteries (veins) do not intersect each other,
- (3) there should be no isolated blood vessel pieces except by concealment.

2.2.1 Initial labeling We can easily give definite labels to some segments using the information concerning their locations and average intensities. We pay attention to the facts that arteries are brighter than veins in general, and arteries often run parallel with veins.

These facts are utilized in our program as follows. Let us refer to Fig. 3 for the explanation.

A search window S is set at the middle point of each line segment i whose length is greater than a given threshold. Another segment k which runs across the window and is parallel to the segment i is selected. If the intensity difference between segments i and k is greater than a certain threshold, the label of artery is given to the segment which is brighter. The label of the other is therefore vein.

As shown in Fig. 3, the intensity of segment i (k) is measured and averaged in the section of length $2W$ centered at the middle point M (N).

With these segments with definite labels, the deterministic labeling might proceed as mentioned in Akita and Kuga⁽⁸⁾. However, some segments are still left unlabeled.

2.2.2 Relaxation labeling In order to give labels to

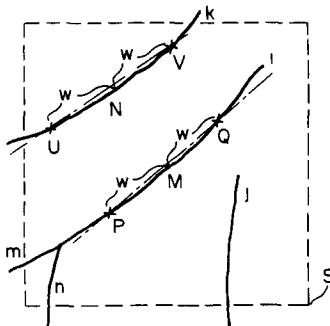


FIG. 3 Segment pairs for initial labeling

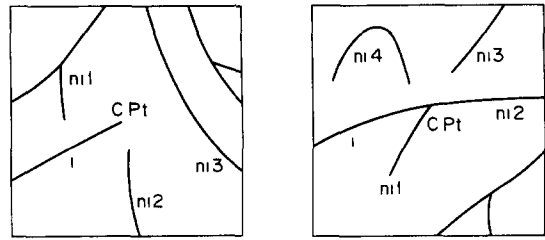


Fig. 4 Neighbors of segment i in R , n_{ij} . The j -th neighbor of i : (a) C Pt, end-point, (b) C Pt, branch-point or cross-point

unlabeled segments by the relaxation method, we first define a neighbor relationship between segments. The neighbors of a line segment i in the area R around each of its characteristic points (C.Pt), i.e. head Pt (H Pt) and tail Pt (T Pt), are defined as follows, and are summarized as the neighbor segment list (NS-LIST).

- (1) When C Pt is an end point. For every other segment j in R , if any end point of j is in R , then j is a neighbor of i . Or if i is extended outwards at C Pt and comes across another segment j in R , then j is a neighbor of i .
- (2) When C Pt is a branch point or a cross point. Every other segment connected to the C Pt and other segments whose end points are in R become neighbors of i .

An example of each situation is shown in Fig. 4, and the contents of the NS-LIST are given below.

NS-LIST on K -th line segment:

- (1) number of neighbor segments at H Pt, $(10m)$ segment number Jhm of m -th neighbor at H Pt, $(10m + 1)$ connectivity between K and Jhm , $(10m + 2)$ distance between K and Jhm ; $(10m + 3)$ angle between K and Jhm , $(10m + 4)$ average intensity difference between K and Jhm ,
 - (101) number of neighbor segments at T Pt, $(100 + 10n)$ segment number Jtn of n -th neighbor at T Pt, $(100 + 10n + 1)$ connectivity between K and Jtn , $(100 + 10n + 2)$ distance between K and Jtn , $(100 + 10n + 3)$ angle between K and Jtn ; $(100 + 10n + 4)$ average intensity difference between K and Jtn .
- Note: Here we assume $0 \leq m \leq 9, 0 \leq n \leq 9$.

Now we formulate the relaxation process.

Let $\Lambda = \{A, V, B\}$, a set of labels, where A, V and B represent artery, vein and others, including unknowns, respectively. For attributes of segment i , we may take the length, the average intensity, the direction at each characteristic point, the average width of the original blood vessel segment, and so forth. Let us represent them by $\alpha(i)$. Then the compatibility function $r_{ij}(\lambda, \lambda')$, where segments i and j have labels λ and λ' , respectively, can be defined as a function of $\alpha(i)$ and $\alpha(j)$. Actually, it is given as a table in which the constraints of blood vessel networks are taken into account. The probability $P_i^k(\lambda)$ that the segment i has the label λ at the k -th iteration satisfies our next equation,

$$P_i^k(A) + P_i^k(V) + P_i^k(B) = 1.0 \quad (1)$$

The contribution coefficient $q_i^k(\lambda)$ to $P_i^k(\lambda)$ at the k -th iteration is defined as,

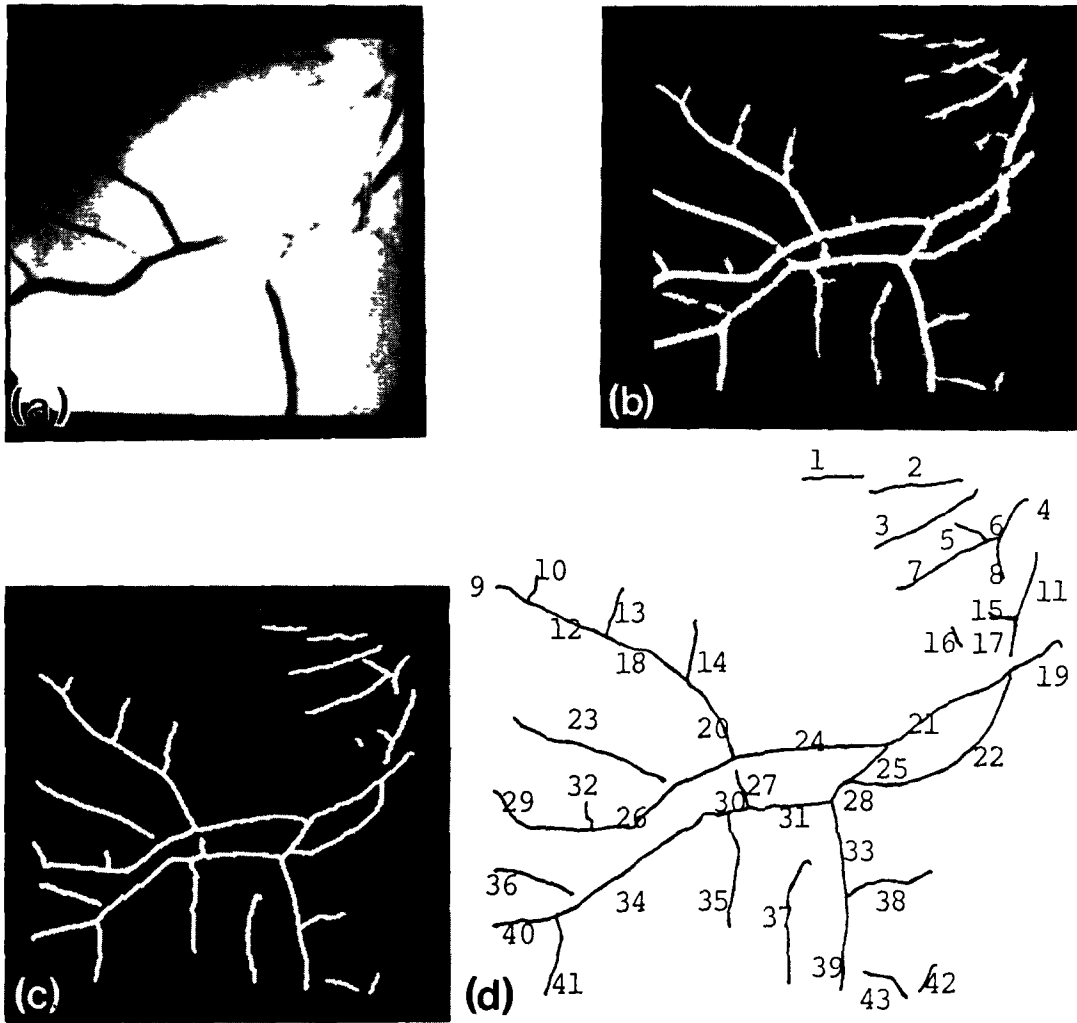


Fig 5 (a) Intensity image, (b) blood vessels, (c) skeleton, (d) numbered skeleton

$$q_i^k(\lambda) = \sum_{j \in N_i} c_{ij} \left[\sum_{\lambda' \in \Lambda} r_{ij}(\lambda, \lambda') P_i^k(\lambda') \right], \quad (2)$$

where N_i is a set of neighbors of segment i and c_{ij} is a coefficient that satisfies

$$\sum_{j \in N_i} c_{ij} = 10 \quad (3)$$

Now the arithmetic updating rule is given as follows,

$$P_i^{k+1}(\lambda) = \frac{P_i^k(\lambda) [1 + q_i^k(\lambda)]}{\sum_{\lambda' \in \Lambda} P_i^k(\lambda') [1 + q_i^k(\lambda)]} \quad (4)$$

The probabilities of some segments are set to 1.0, according to their definite labels given at the initial labeling stage. The initial probabilities $\{P_i^0(\lambda)\}$ of other segments are set as equally probable, and the relaxation goes until some convergence conditions are satisfied.

2.2.3 Verification process According to circumstances, the labels of some segments remain uncertain or inadequate even after convergence. Hence verification or post-processing of the relaxation labeling is

needed. Although the physical level knowledge mentioned before is reflected in the compatibility coefficients to a certain extent, we use it again explicitly to check the labels.

Verification algorithm

- 1 Let the result of the relaxation labeling of segment i be $\{P(L, i), L \in \Lambda\}$ and do the next pre-processing
 - (i) If $P(L, i) = \max_{L \in \Lambda} \{P(L, i)\}$, then $P(L, i) \leftarrow 1.0$ and $P(\bar{L}, i) \leftarrow 0.0$, where \bar{L} stands for all labels except L .
 - (ii) If $P(A, i) = P(V, i) = P(B, i)$, then $P(B, i) \leftarrow 1.0$, $P(A, i) \leftarrow 0.0$ and $P(V, i) \leftarrow 0.0$.
- 2 For every segment except those whose initial labels are definite, examine the terms of contradiction both at its H Pt and its T Pt. When a contradiction occurs, add to the index by one.
- 3 Change label L to label \bar{L} , where $L \neq B$, for every segment whose contradiction index is greater than or equal to one and examine the increase or decrease in the total number TC of contradiction indices. Select the combination of label changing where TC is minimized.

Terms of Contradiction

Let the label of segment i and the set of neighbors at one of its C Pt be $L(i)$ and N , respectively. A contradiction occurs if and only if one of the following cases comes up, assuming that $L(i) \neq B$ and $N \neq \emptyset$ -

- (i) When C Pt is an end Pt or a branch Pt ,
 $L(i) \neq L(j)$ and $L(j) \neq B$ for all $j \in N$
- (ii) When C Pt is a cross Pt ,
 $L(i) = L(j)$ and $L(j) \neq B$ for every j that is in N and connected to C Pt

2.3 Experimental results

We show the V -component (intensity) image, extracted blood vessel image, its skeleton and the sketch of numbered segments in Figs 5(a), (b), (c) and (d), respectively. The sizes of them all are 256×256 pixels. The area R for defining neighbor relationship between segments was set as a square of size 17×17 pixels. The size of R should be determined in consideration of spaces between vessel segments and intermissions on segments, often caused by pre-processing. It is desirable that R is round. We fixed it as square for the brevity of programming. The compatibility function $r_{ij}(\lambda, \lambda')$ was set as a function of the connectivity, the

intensity difference and the angle between segments i and j . It was calculated as a degree of mutual information^(1,3) by the analysis of several color ocular fundus images, and shown as a table of coefficients (Table 1).

It should be noticed that the results of relaxation labeling are sensitive to the compatibility coefficients. We need more statistical analysis of fundus images to get better coefficients.

An experimental result after 100 iterations and the labels after verification are shown in Table 2, together with labeling by eye. The labels of encircled segments in this table were determined at the stage of initial labeling, using only the information of parallelism and intensity difference.

3 DETECTING HEMORRHAGES AND EXUDATES

Hemorrhages and exudates in color ocular fundus images are quite important for the diagnosis of eye diseases and diabetes. Here we propose a detection method for them. They appear as dark or light masses of pixels, so our detection strategy is as follows.

All region boundaries are extracted first. Then blood vessel boundaries are eliminated from them by using

Table 1 Compatibility function
 (1) When segments i and j are connected

		$45^\circ < \theta_{ij} < 135^\circ$		$0^\circ \leq \theta_{ij} \leq 45^\circ$ or $135^\circ \leq \theta_{ij} \leq 180^\circ$	
$\theta_{ij} \leq \delta$	$(A, A) = 0.119$			$(A, A) = 0.129$	
	$(V, V) = 0.191$			$(V, V) = 0.314$	
$\theta_{ij} > \delta$	$(B, B) = 0.0$			$(B, B) = 0.0$	
	$(A, V) = -0.233$	$(V, A) = -0.233$		$(A, V) = -0.406$	$(V, A) = -0.406$
	$(V, B) = 0.0$	$(B, V) = 0.0$		$(V, B) = 0.0$	$(B, V) = 0.0$
	$(A, B) = 0.0$	$(B, A) = 0.0$		$(A, B) = 0.0$	$(B, A) = 0.0$
	$(A, A) = -1.0$			$(A, A) = 0.0$	
	$(V, V) = -1.0$			$(V, V) = 0.0$	
$\theta_{ij} > \delta$	$(B, B) = 0.0$			$(B, B) = 0.0$	
	$(A, V) = 0.301$	$(V, A) = 0.301$		$(A, V) = 0.0$	$(V, A) = 0.0$
	$(V, B) = 0.0$	$(B, V) = 0.0$		$(V, B) = 0.0$	$(B, V) = 0.0$
	$(A, B) = 0.0$	$(B, A) = 0.0$		$(A, B) = 0.0$	$(B, A) = 0.0$

(2) When segments i and j are not connected

		$45^\circ < \theta_{ij} < 135^\circ$		$0^\circ \leq \theta_{ij} \leq 45^\circ$ or $135^\circ \leq \theta_{ij} \leq 180^\circ$	
$\theta_{ij} \leq \delta$	$(A, A) = 0.053$			$(A, A) = -0.018$	
	$(V, V) = 0.388$			$(V, V) = 0.157$	
$\theta_{ij} > \delta$	$(B, B) = -1.0$			$(B, B) = 0.254$	
	$(A, V) = -0.519$	$(V, A) = -0.249$		$(A, V) = 0.079$	$(V, A) = 0.079$
	$(V, B) = -1.0$	$(B, V) = -0.043$		$(V, B) = -0.481$	$(B, V) = -0.481$
	$(A, B) = 0.264$	$(B, A) = 0.102$		$(A, V) = -0.059$	$(B, A) = -0.059$
	$(A, A) = -1.0$			$(A, A) = -0.079$	
	$(V, V) = -1.0$			$(V, V) = -1.0$	
$\theta_{ij} > \delta$	$(B, B) = -1.0$			$(B, B) = 0.155$	
	$(A, V) = 0.264$	$(V, A) = 0.342$		$(A, V) = 0.143$	$(V, A) = 0.222$
	$(V, B) = 0.342$	$(B, V) = 0.268$		$(V, B) = -0.146$	$(B, V) = -0.079$
	$(A, B) = -1.0$	$(B, A) = -1.0$		$(A, V) = -0.021$	$(B, A) = -0.079$

$r_{ij}(\lambda, \lambda') = \beta$ is written as $(\lambda, \lambda') = \beta$ for short
 θ_{ij} , Angle between i and j in R
 θ_{ij} , Average intensity difference between i and j in R
 δ , Threshold for average intensity difference

Table 2 Labeling experiment

Segment no	Labeling by eye	Relaxation labeling			After verification
		A	V	B	
1	B	00	00	10	B
2	B	00	00	10	B
③	V	00	10	00	V
4	B	10	00	00	A
5	B	10	00	00	A
6	B	10	00	00	A
⑦	A	10	00	00	A
8	B	10	00	00	A
9	V	00	10	00	V
10	V	00	10	00	V
11	A	00	10	00	V
12	V	00	10	00	V
13	V	00	10	00	V
14	V	0.863	00	0.137	V
15	B	0.645	00	0.355	V
16	B	0.333	0.333	0.333	B
17	A	00	0.998	0.002	V
18	V	00	10	00	V
19	V	00	0.981	0.019	V
20	V	00	10	00	V
⑳	V	00	10	00	V
㉑	A	10	00	00	A
㉒	A	00	10	00	V
㉓	V	00	10	00	V
㉔	V	00	10	00	V
㉕	V	00	10	00	V
㉖	V	00	10	00	V
27	B	0.906	00	0.094	A
28	A	00	0.706	0.294	V
29	V	00	10	00	V
⑳	A	10	00	00	A
㉑	A	10	00	00	A
32	B	00	10	00	V
㉓	V	00	10	00	V
㉔	A	10	00	00	A
35	B	10	00	00	A
36	A	0.010	00	0.990	B
㉗	A	10	00	00	A
38	V	0.758	00	0.242	V
39	V	00	10	00	V
40	A	10	00	00	A
41	A	10	00	00	A
42	B	10	00	00	A
43	B	0.095	00	0.905	B

A, artery
V, vein
B, unknown

the location information of blood vessel axes obtained in the previous chapter. We also know where the optic discs are by a method that will be introduced later, below. Now from the remaining boundaries we pick up loop-composable sets of edge segments. A loop-composable set may represent an outline of a hemorrhage region or an exudate region. By measuring such parameters as shape, color, size and location, we can recognize which it is. In the following we show some essential processes required for detecting loop-composable sets.

3.1 Extraction of region boundaries

Since fundus images contain minute fluctuations of gray levels caused by noise, differentiation should be

accompanied by smoothing. We use masks and operators, such as shown in Fig. 6. Thus, we obtain differential-value images and direction-code images. Boundary candidates are chosen by scanning these images with a 3×3 window and inspecting the peaks of differential-values and the continuity of direction-codes.

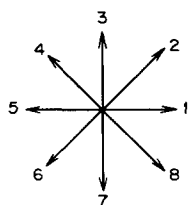
Examples of conditions for the selection of boundary candidate pixel G_0 whose direction code $d_0 = 1$ are shown below (see Fig. 7).

Check the differential value— $G_0 \geq \text{threshold}$

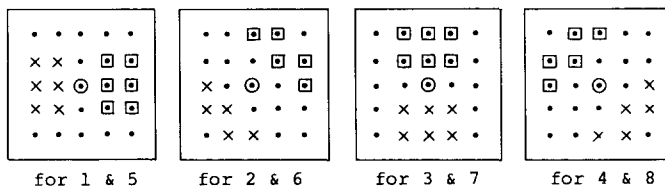
Check the peakness— $G_0 > (G_1 + G_2 + G_3)/3$ and $G_0 > (G_4 + G_5 + G_6)/3$

Check the connectivity of direction—The differences of direction codes between d_0 and those of eight neighbors should be within ± 1 .

(a) direction code



(b) masks



(c) operator

$$G(i, j) = \max_{1 \leq d \leq 8} \{ |S_d(i, j)| \}$$

where $S_5 = -S_1, S_6 = -S_2, S_7 = -S_3, S_8 = -S_4$

$$S_1(i, j) = \left[\sum_{\ell=1}^2 \sum_{k=-1}^1 \{ F(i+k, j+\ell) - F(i+k, j-\ell) \} \right] / 6$$

$$S_3(i, j) = \left[\sum_{\ell=-1}^1 \sum_{k=1}^2 \{ F(i-k, j+\ell) - F(i+k, j+\ell) \} \right] / 6$$

$$S_2(i, j) = \{ F(i-2, j) + F(i-2, j+1) + F(i-1, j+1) + F(i-1, j+2) + F(i, j+2) - F(i+2, j) - F(i+2, j-1) - F(i+1, j-1) - F(i+1, j-2) - F(i, j-2) \} / 5$$

$$S_4(i, j) = \{ F(i-2, j) + F(i-2, j-1) + F(i-1, j-1) + F(i-1, j-2) + F(i, j-2) - F(i+2, j) - F(i+2, j+1) - F(i+1, j+1) - F(i+1, j+2) \} / 5$$

$F(i, j)$: intensity value at (i, j)

Fig 6 Direction-code, masks and the operator for differentiation with smoothing

3.2 Elimination of blood vessel boundaries

Thinning operations and noise removal are performed on the binary images of boundary candidates. The computer traces the boundary patterns and analyzes their structures. The blood vessel boundaries can be discriminated by taking into account the skeletons of blood vessels which were obtained previously. Vessel boundary pairs are chosen under the conditions of

parallelism with vessel axes and expected caliber of vessels

Before describing the details of this process let us define "a boundary sign" of a boundary segment. We assume that the H Pt of an edge segment appears first when scanning goes from upper left to lower right, as in a TV. When an edge segment is traced from its H Pt to T Pt, if we see the darker region on the left hand side

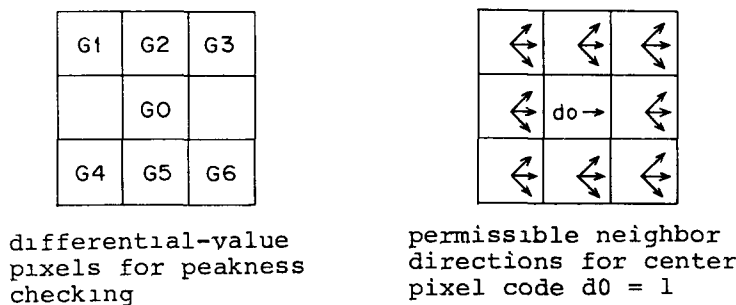


Fig 7 Checking edge candidate for direction-code "1"

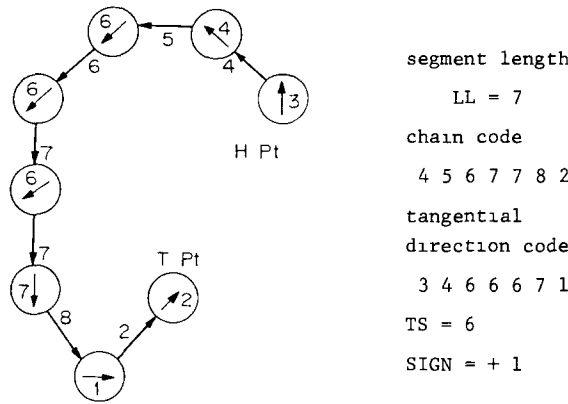


Fig 8 An example of deciding the boundary sign of an edge segment

then its sign is +1 and if we see the brighter region on the left its sign is -1

3.2.1 *Decision of a boundary sign* Starting from the H Pt of a given boundary segment, we calculate the absolute difference (ISA) between the tangential direction-code and the chain-code at each pixel. The tangential direction-code is obtained by the clockwise rotation of the differential direction-code in 90°. Here the chain-code has the same expression as the differential direction code shown in Fig 6(a). In order to consider directional angle difference within 180°, we change ISA to (8-ISA) if it is greater than 4. Sum up ISA along the segment of length LL to get the total amount TS. The sign of this boundary segment is determined as follows

$$TS \leq 2 \quad LL \rightarrow \text{SIGN} = +1$$

$$TS > 2 \quad LL \rightarrow \text{SIGN} = -1$$

An example is illustrated in Fig 8, where circles represent boundary pixels, the arrows in them are tangential directions and the arrows between them stand for chain codes

3.2.2 *How to find blood vessel boundaries* For the discrimination of blood vessel edges from other region boundaries we propose an algorithm such that all boundary segments together with vessel skeleton segments are linearly approximated, and in which pairs of boundary segments which are parallel to vessel skeleton segments and have widths less than a certain threshold are picked up as candidates

We apply a well known line fitting method⁽¹⁴⁾ to the piece-wise linear approximation of segments. (This has been adequately described elsewhere⁽¹⁴⁾) A blood vessel axis segment is approximated by a sequence of

straight line pieces. If we trace it from H Pt to T Pt we can assign a vector to each line piece. Let's take such a vector **c** and call it a vessel axis vector. We show how a corresponding boundary vector **b**, located on the left side of **c**, is found (see Fig 9)

Choose a region boundary segment which is located on the left side of **c** and has the boundary sign indicating that **c** is in the darker area. Consider a sequence of vectors which approximates the segment and each vector of which has the opposite direction to **c**. In Fig 9, points BH and BT have the coordinates (BHC, BHC') and (BTC, BTC'), respectively, in the orthogonal space **cc'**.

$$BHC = \mathbf{h} \cdot \mathbf{c} / |\mathbf{c}|, \quad BHC' = \mathbf{h} \cdot \mathbf{c}' / |\mathbf{c}'|,$$

$$BTC = \mathbf{t} \cdot \mathbf{c} / |\mathbf{c}|, \quad BTC' = \mathbf{t} \cdot \mathbf{c}' / |\mathbf{c}'|,$$

where \cdot and $\|\cdot\|$ represent the inner product and the absolute value of vectors, respectively

The **b** is one of these vectors and satisfies the following conditions

- (1) $0 \leq BTC' \leq w$ and $0 \leq BHC' \leq w$, where w is a half of the expected caliber of blood vessels
- (2) $0 \leq BHC \leq |\mathbf{c}|$ or $0 \leq BTC \leq |\mathbf{c}|$ or $(BHC > |\mathbf{c}| \text{ and } BTC < 0)$
- (3) $\mathbf{b} \cdot \mathbf{c}' / |\mathbf{b}| |\mathbf{c}'| \leq \cos(180^\circ - \gamma)$, where γ is an allowance of angle to detect parallelism

On the other hand, when we find a corresponding vessel boundary vector located on the right side of **c**, we seek for a region boundary segment which is on the right hand side of **c** and has the boundary sign indicating that **c** is in the darker area, and we follow the same process mentioned above

Thus the sequences of vectors that fit blood vessel boundaries are chosen. In this way we can easily separate them from region boundaries

3.3 Detection of loop-composable sets of edges

Hemorrhages and/or exudates appear as dark and/or light masses of pixels outside the blood vessel regions. In the images of region boundaries they are

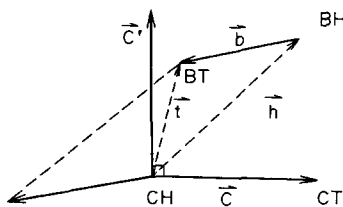


Fig 9 Judgement of left-side vessel boundary segment

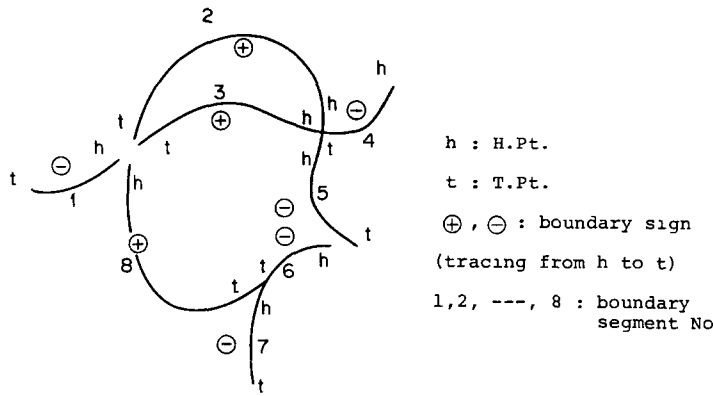


Fig 10 An example of detecting a loop-composable set of boundary segment

considered as loop-composable sets of boundary segments. A loop-composable set consists of edges whose boundary signs coincide when they are traced in a certain direction (clockwise or counter-clockwise). Note that the sign of a boundary should be changed to the opposite when it is traced from T Pt to H Pt.

Detection algorithm 1
 On the image of region boundaries where vessel edges have been eliminated, carry out the following steps

- 1 Pick up the I -th boundary segment and check whether there are neighbors around its C Pt or not. If not, go to 4.
- 2 Select one of the neighbors that has the minimum intensity difference between I and whose boundary sign coincides with that of I . Let it be J and register it in the set Z . If there is no such J , erase the content of Z and go to 4.
- 3 Do as above with J , and continue. If a selected segment in this process has already been registered in Z , then go to 4.
- 4 The detection process on the I -th segment ends. If Z is not empty, it is a candidate for a loop-composable set. The algorithm can be intuitively understood if we take a look at Fig 10. In this example, $Z = \{3, 5, 6, 8\}$ becomes a candidate since all the segments in Z have the same boundary sign, -1 , when they are traced clockwise, which means that the region surrounded by Z is darker than outside. It is expected that the region is a hemorrhage.

3.4 Experimental results

A result of each step in the above mentioned process is shown by the photograph in Fig 11. The size of each image is 256×256 pixels, and that of the search window for neighbor boundary segments is 13×13 pixels. The computer program for detecting loop-composable sets is more elaborate than the algorithm stated briefly in the previous section, because we have to exclude such a set that consists of one short, open segment whose shape is not round or in which the last component is so short that both of its C Pt are in the search window. There remain a few pieces of vessel

edge in Fig 11(f) and Fig 11(g) because of the failure to find vessel boundary pairs at these positions.

4. LOCATING OPTIC DISCS

The optic disc is the entrance region of the veins and arteries onto the retina. It is the most conspicuous part in the fundus since it is brighter than the outskirts and its shape is round. Its diameter is often used as the standard to measure distances and sizes in the fundus image. For example, the fovea lies about 2.5 disc diameters away from the disc center. Thus, the detection of the disc's location is fundamental to an understanding of fundus images. We propose a detection algorithm as follows, utilizing the above knowledge.

Since a retinal blood vessel comes from the disc, if we can define the parent-child relationship between line segments at branch points, it will be possible to trace back to the root, i.e. to the disc. There are also some characteristic points in that area and the average intensities of non-vessel pixels in the windows centered around those points may generally be greater than those of the windows at other characteristic points. The detection algorithm selects one of these to indicate the disc position.

Before stating the algorithm, we define two notions: vessel intensity near a branch point and a parent segment. The former is the average intensity of vessel pixels on the line segment which are closer than d from the branch point (See Fig 12). Let the three segments which meet at a branch point be $L1, L2$ and $L3$. Let the intensity difference and the angle between two segments i and j be G_{ij} and A_{ij} , respectively. Then the parent segment LP is defined as follows:

Let $a_0 = \min(A_{12}, A_{23}, A_{13})$. If G_{12}, G_{23} and G_{13} are less than or equal to ρ_0 , and if

- (i) $A_{12} = a_0$ and $A_{12} < 90^\circ$, then $LP = L3$.
- (ii) $A_{23} = a_0$ and $A_{23} < 90^\circ$, then $LP = L1$.
- (iii) $A_{13} = a_0$ and $A_{13} < 90^\circ$, then $LP = L2$.

Detection algorithm 2

- 1 Calculate the average intensity of non-vessel pixels in the window at each C Pt using CP-

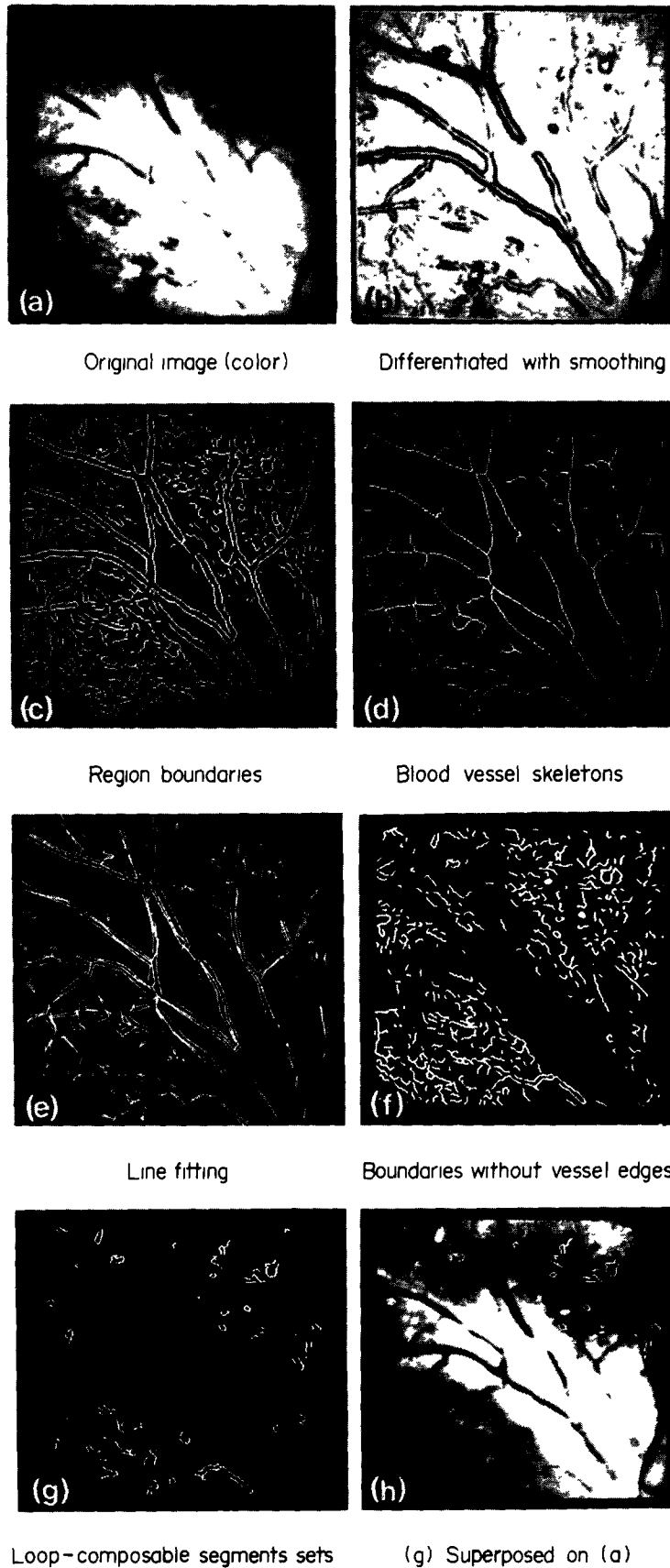


Fig 11 A process of locating hemorrhages and exudates

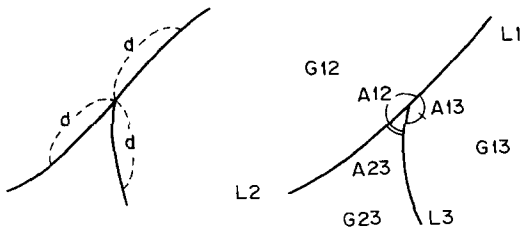


Fig 12 Definitions of a vessel intensity near a branch point and a parent segment

LIST, LS-LIST, the binary vessel image and the intensity image

2 Selection of candidate points

- (1) When there exists a branch point with 0-flag in the process completion table, this means that it is not processed yet. Do the following
 - (a) If G_{12} , G_{23} and G_{13} are less than or equal to ρ_0 , then determine the parent segment LP and set 1 to the flag of this branch point in the process completion table. Look at the other CPt of LP . If it is a branch-point, then go back to (a). If it is an end-point, register it in the candidate table.
 - (b) If any one of G_{12} , G_{23} and G_{13} is greater than ρ_0 , then set its flag to 1 in the process completion table.
 - (c) Check the candidate table. If the number of the registered points is less than two or

the minimum distance among them is greater than D , then go to 2-(2). Otherwise, select the point which has the maximum average intensity as the candidate and go to 3 (D is a standard of the disc diameter).

- (2) When there exists no significant branch-point, choose NC Pt with greatest average intensities and go to 3-(1).

3 Consider the NC Pt in the area of size S around the candidate and do the following (S is a standard of the circumscribed quadrilateral of the disc)

- (1) Choose the central point P_c such that

$$P_c = \left\{ P_j \mid \min_j \right.$$

$$\left. \times \left[\sum_{i=1}^N \sqrt{(x_i - x_j)^2 + (y_i - y_j)^2} / (N - 1) \right] \right\}$$

- (2) Exclude those points whose distance from P_c is greater than d .
- (3) Among n points chosen by the above mentioned steps, select one which has the maximum average intensity. This is the disc representative point.

Two experimental results of the algorithm are shown in Fig 13, where we set $d = 10$, $\rho_0 = 10.0$, window size = 16×16 pixels, $D = 16\sqrt{2}$ and $S = 33 \times 33$ pixels. The size of each image is 256×256 pixels.

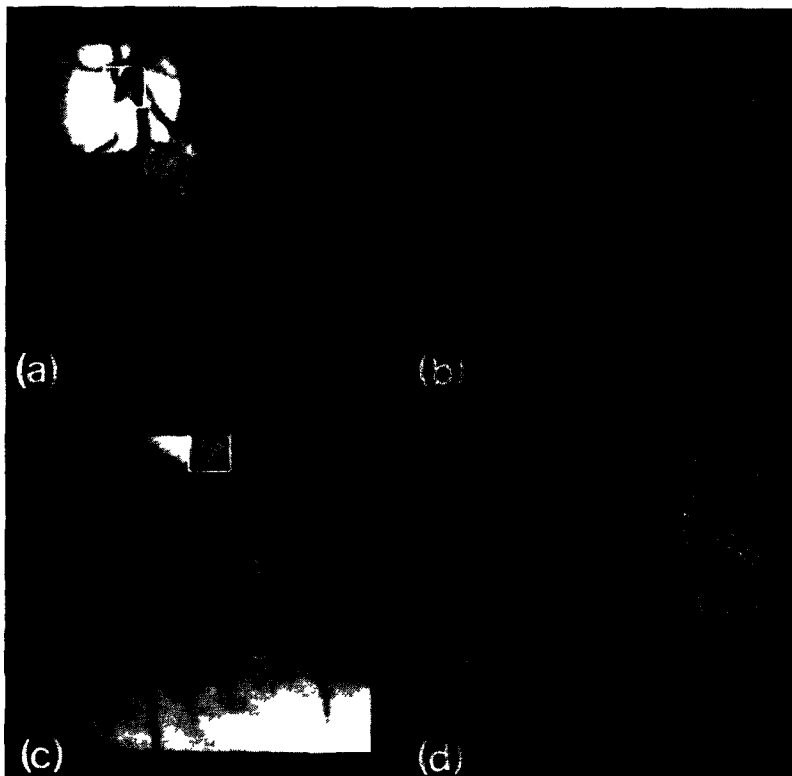


Fig 13 Locating optic discs (a) and (c), Intensity images and detected position of discs indicated by squares, (b) and (d), blood vessel skeletons

5. CONCLUSION

Here we present a brief comment on the computer analysis of arterio-venous (A-V) crossing phenomena which are utilized for ranking hypertension

Medical doctors pay particular attention to the calibers and shapes of veins at crossings. In order to automate this process it is essential that the computer can locate A-V crossings. The algorithm for this is easily derived from the discussion in Section 2.2. Namely, find branch-points or cross-points where segments of different label meet. These will be the location of A-V crossings. Akita and Kuga⁽⁹⁾ have already proposed a procedure for measuring the running states of veins at crossings such as meandering, banking and tapering.

This work was done from the viewpoint of digital image processing and artificial intelligence. It does not yet include the automatic diagnosis of diseases, which is left for the future.

SUMMARY

We have studied some fundamental problems towards the understanding of color ocular fundus images which are used in the mass diagnosis of adult diseases such as hypertension and diabetes.

These problems are the extraction of blood vessels from the retinal background, the recognition of arteries and veins and the detection and analysis of peculiar regions such as hemorrhages, exudates, optic discs and arterio-venous crossings.

First of all, we have analyzed the chromatic properties of color ocular fundus images to obtain signal level knowledge on retinas, discs, arteries, veins, hemorrhages and exudates.

We then applied a line detection algorithm, which was used to find linearments such as roads and rivers in satellite imagery, so as to extract the blood vessels and make skeleton patterns of them and analyze and describe their structures. The computer also detects characteristic points and lists vessel line segments. Several parameters on each of these are measured.

For the recognition of line segments of arteries and/or veins in the vessel networks we show an initial labeling scheme and describe how to apply a relaxation method, together with a verification process for them. First, a few segments which satisfy a certain constraint are picked up and discriminated as arteries or veins. Then the remaining unknown ones are labeled by the relaxation method. Finally the label of each line segment is checked and corrected so as to minimize the total number of labeling contradictions.

For the detection of hemorrhages and exudates we define loop-composable sets of edge segments which are separated from region boundaries. Since the regions of hemorrhages/exudates consist of dark/light masses of pixels, loop-composable sets of region boundary segments are quite useful for locating them

in the fundus images, which include shading of unevenness of light intensity.

In order to locate optic discs we define a parent-child relationship between blood vessel segments and propose an algorithm that traces vessel tree branchings back to their roots.

We utilize the fact that the disc is the entrance of veins and arteries onto the retina and that it is generally brighter than its surroundings.

In order to achieve a computer analysis of arterio-venous crossing, it is essential that the computer can locate the crossings. This becomes possible by means of the above mentioned processes. We have already proposed an automatic procedure for measuring the states of veins at crossings in another paper.

Some experimental results of these proposed methods are also presented.

Acknowledgement—This research was supported by the Pattern Information Processing System Project of the Agency of Industrial Science and Technology of the Ministry of International Trade and Industry of Japan.

REFERENCES

- 1 J Parr, *Introduction to Ophthalmology* Oxford University Press, Oxford, U.K. (1978)
- 2 H Kabayama, *Atlas of Fundus Photography* Homeido, Tokyo (1975)
- 3 B H McCormick, J S Read, R T Borovec, R C Amendola and M H Goldbaum, Image processing in television ophthalmoscopy, *Digital Processing of Biomedical Images*, p 399 Plenum Press, New York (1976)
- 4 S Tamura, K Tanaka, M Hashi, S Omori, A Okada, M Inoue and K Okasaki, Analysis of fluorescence fundus angiographies, *National Convention of IPSJ*, 673-674 (1977)
- 5 M Tanaka and K Tanaka, An automatic technique for fundus-photograph mosaic and vascular net reconstruction, *Proceedings of MEDINFO-80*, 116-120 (1980)
- 6 P A Nagin and B Schwartz, Approaches to image analysis of the optic disc, *Proceedings of the 5th IJCPR*, 948-956 (1980)
- 7 S Yamamoto and H Yokouchi, Automatic recognition of color fundus-photographs, *Digital Processing of Biomedical Images*, p 385 Plenum Press, New York (1976)
- 8 K Akita and H Kuga, Towards understanding color ocular fundus images, *Proceedings of IJCAI-79*, 7-12 (1979)
- 9 K Akita and H Kuga, Digital processing of color ocular fundus images, *Proceedings of MEDINFO-80*, 80-84 (1980)
- 10 W K Pratt, *Digital Image Processing* Prentice-Hall, Englewood, New Jersey (1978)
- 11 G J Vanderbrug, Line detection in satellite imagery, *IEEE Trans Geosci Electron GE-14*, 37-44 (1976)
- 12 A Rosenfeld, R A Hummel and S W Zucker, Scene labeling by relaxation operations, *IEEE Trans Syst Man Cybernet* 433 SMC-6, 420-433 (1976)
- 13 S Peleg and A Rosenfeld, Determining compatibility coefficients for curve enhancement relaxation processes, *IEEE Trans Syst Man Cybernet SMC-8*, 548-555 (1978)
- 14 R O Duda and P E Hart, *Pattern Classification and*

Scene Analysis, p. 338. John Wiley & Sons, New York (1973) 15 T. Kanade, Region segmentation: signal vs. semantics, *Proceedings of the 4th IJCNN*, 96–105 (1978)

About the Author—KOICHIRO AKITA received the B.S.E.E. degree from the University of Tokyo in 1968 and the M.S.E.E. degree from the University of Southern California in 1976. He is a senior research engineer at the Central Research Laboratory of the Mitsubishi Electric Corp. His research interests are in image processing and artificial intelligence.

About the Author—HIDEKI KUGA is a research engineer at the Central Research Laboratory of the Mitsubishi Electric Corp. He received the B.S.E.E. and the M.S.E.E. degrees from Kyushu University in 1975 and in 1977, respectively. He is now interested in pattern recognition and robotics.